Available online at www.sciencedirect.com

ScienceDirect

Energy Reports 7 (2021) 430–439

www.elsevier.com/locate/egyr

17th International Symposium on District Heating and Cooling, DHC2021, 6–9 September 2021, Nottingham, United Kingdom

# A comparison of prosumer system configurations in district heating networks

Daniel Zinsmeister[a,*], Thomas Licklederer[a], Franz Christange[b], Peter Tzscheutschler[a], Vedran S. Perić[a]

[a] *Technical University of Munich, 80333 Munich, Germany*
[b] *Triowatt GmbH, 83071 Stephanskirchen, Germany*

Received 4 August 2021; accepted 7 August 2021

**Abstract**

Prosumer-based district heating networks attract an increasing interest in energy research. There are numerous publications addressing the prosumer integration into district heating networks with a focus on grid side operation. However, the operation of the prosumer side has not been extensively investigated in the literature where bidirectional heat transfer stations, heat generators, consumption and storages can be connected in different ways. These different connections have different influences on the district heating network operation that require deeper analysis and understanding.

This paper evaluates the influence of using different prosumer side system configurations as well as their suitability for prosumer-based district heating networks. Beginning with the characteristics of possible prosumer side configurations this paper evaluates the applicability of these configurations according to the number of components and operational flexibility. Subsequently, the most promising subset of the evaluated configurations are simulated in realistic scenarios using SimulationX® software and its Green City toolbox to gain detailed insight into their operation and efficiency. The simulated configurations are analyzed with respect to exportable excess heat, grid temperatures and the overall efficiency of the heat supply. The configurations are studied in various scenarios that differ in heat generation type (heat pump, solar thermal collectors or combustion device) and the necessary supply temperatures on the prosumer and grid side.

In conclusion, this paper provides a decision guidance to select the most suitable prosumer side configuration for a desired district heating network and consumption temperatures.


Peer-review under responsibility of the scientific committee of the 17th International Symposium on District Heating and Cooling, DHC2021, 2021.

*Keywords:* District heating; Prosumer; Decentralized feed-in; Heat system configurations

## 1. Introduction

In order to reach the climate change goals of the Paris agreement, all energy sectors have to reduce their emissions drastically, including the heating sector. Within the heating sector, district heating and cooling grids

* Corresponding author.
*E-mail address:* zinsmeister@tum.de (D. Zinsmeister).

https://doi.org/10.1016/j.egyr.2021.08.085


Peer-review under responsibility of the scientific committee of the 17th International Symposium on District Heating and Cooling, DHC2021, 2021.

**Nomenclature**

| | |
|---|---|
| 3WV | 3-way valve |
| CG | Combustion-based heat generators |
| DH | Bidirectional district heating station |
| DHW | Domestic hot water |
| HC | Heating consumption |
| HG | Heat generation |
| HP | Heat pump |
| LTDH | Low temperature district heating |
| ST | Solar thermal collectors |
| TS | Thermal storage |
| ULTDH | Ultra low temperature district heating |

are one promising aspect to reduce emissions [1]. District heating grids were introduced in the 19th century and have evolved since then from high temperature steam grids to modern, low temperature systems, increasing their efficiency step by step [2].

One possibility to further reduce the CO2 emissions of district heating system is to integrate prosumers. Prosumers are market participants, who can produce and consume energy. In district heating grids, prosumers can feed excess heat into the district heating grid, or extract heat from the grid, if it is more economic for them [3]. The excess heat ideally comes from low emission heat generators, such as solar thermal collectors, heat pumps or combined heat and power units. The integration of prosumers or a decentralized heat supply can also reduce heat losses due to lower transport distances [4]. The potential of prosumer based district heating stations is high especially in areas with mixed building stocks [5].

Decentralized feed-in to the district heating grid results in several effects, not considered in standard district heating grids. The decentralized feed-in can lead to a local drop of the supply temperature and a locally increased flow velocity [3]. Also, the flow direction within the district heating grid can change due to different feed-in points, resulting in a supply frontier in which there is no flow and thus the temperature drops, leading to stronger thermal stress of the pipes [6]. This might require a transformation of today's district heating networks into smart district heating networks [3].

The integration of heat from prosumers demand a new approach for the district heating substation, especially since different heat sources often require individual concepts. For the utilization of low temperature waste heat, a heat pump can be used in the heat transfer station to raise the low temperature level of waste heat to the necessary heat network temperature [7]. Decentralized heat pumps can also be used directly to substitute existing heat generators in heat networks [8]. Another possibility for the use of heat pumps in the transfer station are so-called booster heat pumps. This offers the possibility of using very low heat network temperatures. If heating and cooling are used simultaneously, the waste heat or cold of the heat pumps can also be used very effectively by means of intelligent control [9,10]. Several other publications discussed the integration of solar thermal collectors into prosumer-based district heating systems. On the grid side, the three possible feed-in types are 'return to flow', 'return to return' and 'flow to flow', of which 'return to flow' is the option, chosen as the best by Mangold et al. [11]. Rosemann et al. shows a control algorithm for a prosumer substation with solar thermal collectors, where the consumption side connects both the collectors and the district heating grid [12]. Another approach is presented by Lamaison et al. and Paulus et al. where the district heating substation works as hydraulic switch, connecting the consumer, the solar thermal collectors and the district heating grid [13,14].

The above referenced publication made good progress with the prosumer district heating connection, however their common assumption was a system without a storage. Nevertheless, can the introduction of a storage be beneficial for heat prosumers because of the increased flexibility, especially for small scale district heating grids. When using a storage, the number of possible combinations rises dramatically.

The influence of the house side of heat prosumers has not been studied to the best of our knowledge. Therefore, this paper investigates which combination is best suited for different heat prosumers. First, the different components heat generators (HGs), heating consumption (HC), the district heating substation (DH) and the thermal storage (TS) are characterized. Based on this characterization, various configurations are defined for a scenario analysis. This scenario analysis simulates configurations with the different HG types heat pump (HP), combustion-based heat generator (CG) and solar thermal collectors (ST). The results are used to rate the configurations and offer a guidance to select the most suitable prosumer side configuration.

## 2. Prosumer system components

In this chapter, the different prosumer system components are described and possible restrictions for the usage in a prosumer system are highlighted.

### 2.1. Heat demand

The heat demand consists of HC and domestic hot water (DHW) consumption.

HC can be classified into two temperature levels: Radiator panel heating, where the supply and return temperature is 60 °C and 45 °C respectively and surface heating, where the temperature is 40 °C and 30 °C respectively. The supply temperature of the HC is controlled by a mixing station to provide a constant temperature for the heating system. The flow rate is controlled by a thermostat.

In order to decouple the DHW demand from the heat production, the DHW consumption is directly linked to the TS. To prevent problems with legionella, the temperature of the DHW reservoir is restricted, e.g. the German standard requires DHW to be heated to 60 °C or higher for DHW systems with a total content of more than 3 l [15].

### 2.2. Thermal storage

The integration of several TS tanks was excluded since heat systems normally only have one TS and to keep the number of variants manageable. The TS can have several connections at different heights. This improves the temperature layering within the TS, so that for example water layers with high temperature are at the top separated from colder water layers and thus preventing exergy losses by the mixing of hot and cold water. The temperature layering can be maintained very well during operation if loading and unloading is done correctly [16]. The temperature of the TS can be measured at different height levels.

In order to fulfill the hygienic requirements, the DHW circuit and TS are separated with an internal or external heat exchanger. Fig. 1 shows the two possible DHW integrations.

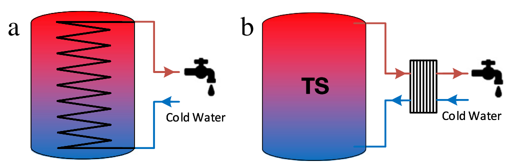


**Fig. 1.** DHW storage integration (a) with external heat exchanger, (b) with internal heat exchanger.

### 2.3. District heating substation

The focus of this paper are district heating systems with low supply temperatures, which Østergaard et al. classified as low-temperature district heating (LTDH) with supply temperature range between 50 °C and 65 °C and ultra low temperature district heating (ULTDH) with a supply temperature range between 30 to 50 °C [17].

These temperature ranges define possible configurations. LTDH are able to provide a temperature level that fulfills DHW demands and can thus be combined with high and low temperature HC and/or directly to the TS. ULTDH in contrast cannot provide heat fulfilling DHW demands and requires an additional HG.

### 2.4. Heat generators

For the comparison of prosumer system configurations, HGs are divided into three subgroups:

- HP, which have a constant temperature difference between supply and return temperature;
- volatile ST and
- CG with a controllable supply temperature.

*Heat pumps:*
With rising supply temperatures, the efficiency of HPs decreases. For this reason, the internal control of standard HPs does not allow influencing the supply temperature directly, but runs at a constant temperature difference between supply and return temperature to maximize the efficiency. In order to reach high supply temperatures, e.g. for DHW, the return temperature has to increase accordingly. This can be done best by using the layering of the TS and extracting the return water from a higher, warmer storage level.

When connecting the HP to the TS, two 3-way valves (3WV) are used to switch between low and high temperature operation. Fig. 2 shows a common configuration without the connection to DH according [18].

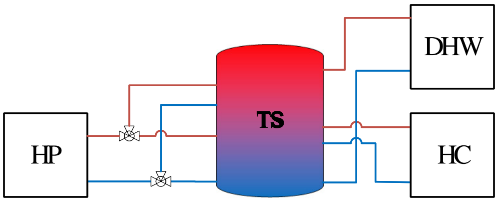


**Fig. 2.** Common HP integration.

Due to the bad efficiency of HPs at high temperature, only low temperature HC is considered.

*Solar thermal collectors:*
In contrast to other HG units, ST is a volatile HG, which means, it cannot be used as a single heat source. In order to prevent ST from freezing during winter, antifreeze is added. This requires ST to be in a separate circuit, where the heat is transferred with a heat exchanger, normally done in small heating systems with an internal heat exchanger within the TS.

*Combustion-based heat generators:*
The supply temperature of CG, like condensing boilers or combined heat and power, can normally be controlled directly and has little influence on the efficiency of the heat generation. The efficiency of a CG is mostly dependent on the return temperature and rises due to the condensing effect, if the return temperature is lower.

## 3. Prosumer system combinations

The possible prosumer system combinations can be divided into three categories:

- Parallel combinations, where all elements are connected to the TS;
- Serial combinations, where three elements are connected in series;
- Mixed combinations, where parallel and serial features are realized.

An overview and preliminary characterization of 14 possible combinations is published separately [19]. Fig. 3 shows the 9 combinations that were chosen for further investigation. The other combinations were excluded due to high estimated exergy losses, too little flexibility or because they are not usable in prosumer-based district heating grids.

The combinations can be evaluated by the following criteria:

- Costs, related to the number of necessary components like pumps and valves or if special components have to be used.
- Operational flexibility, defined by the flexibility to switch between heat extraction and feed-in and the flexibility of controlling the feed-in temperature and power.

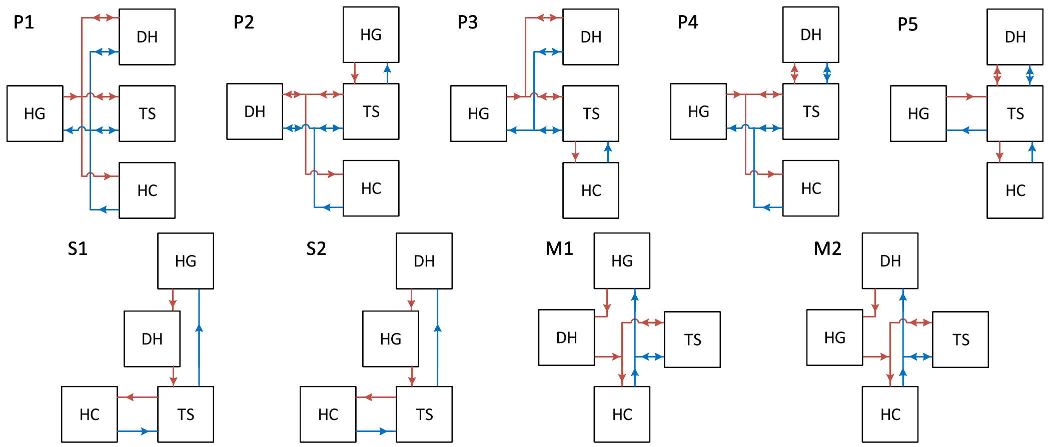


**Fig. 3.** Parallel combinations (P1 to P5), serial combinations (S1 and S2) and mixed combinations (M1 and M2).

## 4. Scenario analysis

The combinations presented in the previous chapter are evaluated using a scenario analysis to identify the configuration best suited for different heat prosumers. For this purpose, the configurations are simulated for the different cases ‘extraction’, ‘no grid’ and ‘feed-in’.

### 4.1. Simulation model

In order to assess the performance of different prosumer side configurations, they are simulated using the SimulationX® software. SimulationX is based on the modeling language Modelica. The integrated Green City library provides a wide range of component models of state-of-the-art energy supply systems, including detailed models of thermal components [20]. Most elements of the Green City library are accessible, thus making it possible to customize individual simulation blocks. Pipe losses and insulation are neglected for the model as these are specific to individual constructions and the paper aims at deriving general conclusions on the investigated configurations.

For the simulation, existing TS and HC models where used. The three different HG models were derived and the control strategy of Section 4.2 was implemented. The DH simulation block was split into a DH-feed-in block and a DH-extract block. Fig. 4 presents the framework of one prosumer system configuration.

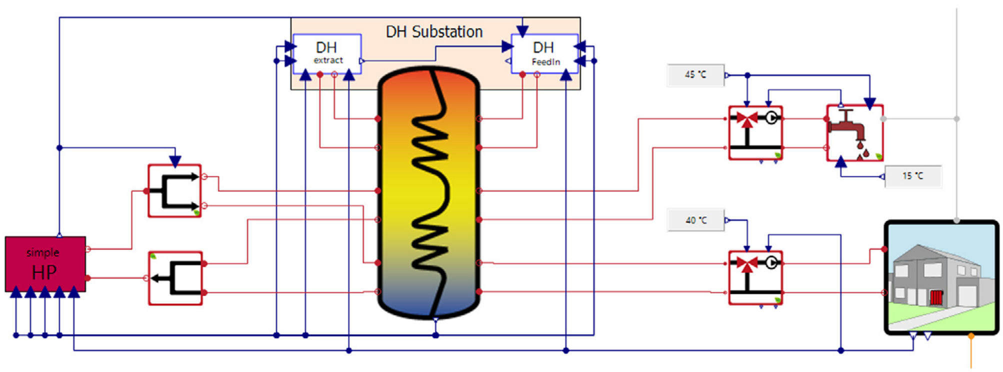


**Fig. 4.** Model of a prosumer with a HP and the configuration P5.

### 4.2. Control strategy

The control strategy of the DH was based on the strategy of Rosemann et al. [12], where the volume flow of the pump on the prosumer side operates with a constant flow rate. The flow rate on the grid side is controlled to reach the supply temperature on the prosumer side when extracting heat and to reach the supply temperature of the grid side when feeding in. When classifying the feed-in potential, the control strategy tries to feed in as much heat as possible.

The criteria for feed-in or extraction are:

- Feed-In:
  Switched on: $T_{storage,top} > 60\ °C + \Delta T$ and $T_{storage,middle} > 40\ °C + \Delta T$
  Switched off: $T_{storage,top} < 60\ °C$ or $T_{storage,middle} < 40\ °C$
- Extraction:
  Switched on: $T_{Storage,top} < 55\ °C$ or $T_{Storage,middle} < 40\ °C$
  Switched off: $T_{Storage,bottom} > 55\ °C/40\ °C$

Information about the control strategy of HG is difficult to assess, since most manufacturers do not share their individual control strategy. For this reason, a relatively simple control strategy is chosen, which only considers the temperature of the TS at different layers, which to our knowledge represents a common control philosophy for HGs, as for example implemented at [21]. Since the purpose of the scenario analysis is to determine the potential of the different configurations independent of the control strategy, a simple and similar control strategy between the different HG types is beneficial. The control strategies are implemented as follows

Heat pump (HP):

- Switched on with $T_{sup,high}$ when $T_{Storage,top,HPin} < 60\ °C$, switch off when $T_{Storage,top,HPout} > 60\ °C$
- Switched on with $T_{sup,low}$ when $T_{Storage,middle} < 40\ °C$, switch off when $T_{Storage,bottom} > 40\ °C$
- If the switch on conditions for $T_{sup,low}$ and $T_{sup,high}$ are true, $T_{sup,high}$ is produced.
- The volume flow is controlled to have a temperature difference of 10K between $T_{sup}$ and $T_{ret}$.

Combustion-based heat generator (CG):

- Switched on when $T_{Storage,top} < 60\ °C$ or $T_{Storage,middle} < 40\ °C$, switch off when $T_{Storage,bottom} > 60°$
- The volume flow is controlled to have a constant supply temperature of 70 °C.

Solar thermal collectors (ST):

- The ST pump is switched on, when the collector temperature is bigger than the TS inlet temperature.
- The volume flow is controlled to reach the specified supply temperature or switched off, if the TS reaches its maximum temperature.
- The supply temperature is defined as $T_{sup} = 60\ °C$ if the TS inlet temperature is lower than 60 °C to provide water for DHW as efficient as possible. When the inlet temperature is above 60 °C, $T_{sup}$ is changed to 80 °C to further charge the TS.

In order to reduce losses during summer, when no heating, but only DHW is required, the TS is only charged at the top half.

### 4.3. Scenario cases

The scenarios are simulated for a whole year. The HC is defined by a five-person household with different temperature levels: 40/30 °C (HC low) and 60/45 °C (HC high) according to 2.1. The DHW consumption is used according to the model of Jordan et al. [22]. The TS has a volume of 750 l and an internal heat exchanger for DHW and ST, if used.

The HG are sized to cover the load of the building:

- HP: 10 kW at $T_{sup} = 40\ °C$
- CG: 10 kW
- ST: flat plate collector with 12 $m^2$ collector surface

As described in 2.3, two different temperature levels where assumed for the DH grid. ULTDH with a supply temperature of 45 °C and LTDH with a supply temperature of 65°.

In order to classify each configuration, the scenarios are run in three different operation phases:

- No Grid:
  In this case, the heat is provided solely by the HG and is neither fed into the grid nor extracted from it in order to determine the efficiency of the configuration.
- Feed-In:
  For the case of feed-in, the potential of the configurations to provide heat to the grid will be assessed. In order to make a preselection for further holistic studies, we only examine the prosumer side possibilities in this paper. Therefore, the maximum, grid-independent feed-in potential is calculated and the HG is operated as constant as possible in order to feed as much heat as possible into the grid. In reality, however, the feed-in is strongly dependent on the current grid conditions. The return temperature of the grid is assumed in this scenario constant at 45/30 °C
- Extraction:
  In the extraction scenario, the demand should be covered by the heating network. When using ULTDH, the HG can support to provide the temperature level required for DHW.
  In this scenario, the grid supply temperature is assumed constant at 65/45 °C.

### 4.4. Evaluation

For each operation phase, the efficiencies are evaluated. When no grid is connected, the efficiency $\eta_{no\,grid}$ is calculated based on the heat demand $E_{Demand}$ and the fuel consumption of the HG $E_{fuel,no\,grid}$:

$$\eta_{no\,grid} = \frac{E_{Demand}}{E_{fuel,no\,grid}} \tag{1}$$

The feed-in potential is described by the total amount of energy, fed into the grid over the year $E_{feed\,in}$. The feed-in efficiency $\eta_{feed-in}$ is calculated on basis of the additional fuel amount necessary to produce $E_{feed-in}$. For the additional fuel amount, $E_{fuel,no\,grid}$ is subtracted from the fuel amount of the feed-in scenario $E_{fuel,feed-in}$:

$$\eta_{feed-in} = \frac{E_{feed-in}}{E_{fuel,feed-in} - E_{fuel,no\,grid}} \tag{2}$$

When extracting heat from the grid, the return temperature should be as low as possible. Therefor the average grid return temperature $T_{ret,grid}$ is important to evaluate the configuration. Another criterion is the extraction efficiency, which can be calculated by dividing $E_{Demand}$ by the amount of energy, extracted from the grid $E_{extraction}$ plus the fuel amount $E_{fuel,extraction}$, if necessary.

$$\eta_{extraction} = \frac{E_{Demand}}{E_{extraction} + E_{fuel,extraction}} \tag{3}$$

## 5. Results

All simulation results are published in more detail in [19].

Fig. 5 shows the results of all configurations using a CG. In this case, configuration P1 is in general the best choice. With this configuration the highest degree of flexibility is obtained, since the feed-in and consumption temperature level does not depend on the TS condition, but can be directly influenced. Due to low return temperature on the prosumer side and low TS losses, the efficiency for ‘no grid’ and ‘extraction’ are best and the return temperature on the grid side during ‘extraction’ is lowest. Since the ULTDH grid cannot provide heat that meets the temperature requirements of DHW, the CG must generate the necessary heat in this case as shown in Fig. 5c.

If the goal is to achieve the highest possible feed-in, configuration S1 might be interesting for the CG at a low temperature level of the HC (blue scenario). Another advantage is that fewer components are needed, which saves costs. However, the flexibility for ‘feed-in’ is limited, since this is only possible when the CG is active and the TS is sufficiently filled for the DHW demand. The high return temperature during ‘extraction’ is another disadvantage.

When using a HP, only P2, P5 and P5* are possible, since it must be connected directly to the TS. P5* is the same configuration as P5 but with an additional 3WV in the return line, so that the return flow of the DH can be

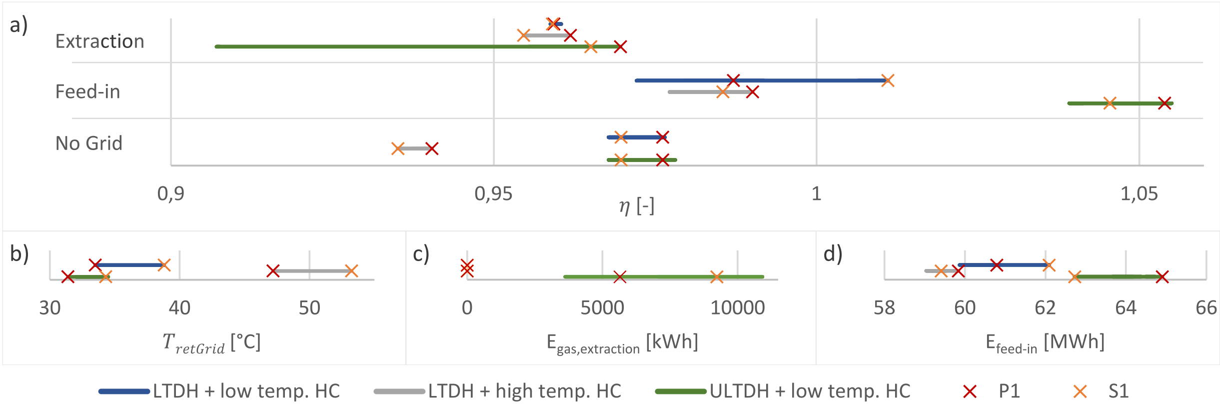


**Fig. 5.** Simulation results of the CG: Results lie in the range indicated by the different lines; the line color represents different scenarios; two promising configurations, P1 and S1, are marked separately. (a) shows the efficiency for the different operation phases 'extraction, 'feed-in' and 'no grid', (b) shows the averaged return temperature during 'extraction', (c) the additional gas power necessary for the CG to heat up water to DHW temperature when the grid is too cold for 'extraction' and (d) shows the maximum feed-in potential during 'feed-in'. . (For interpretation of the references to color in this figure legend, the reader is referred to the web version of this article.)

fed in at different TS heights. Fig. 6 shows the results for this generator. The efficiency for the scenario 'no grid' is the same for both configurations with an averaged efficiency (COP) of 3.83.

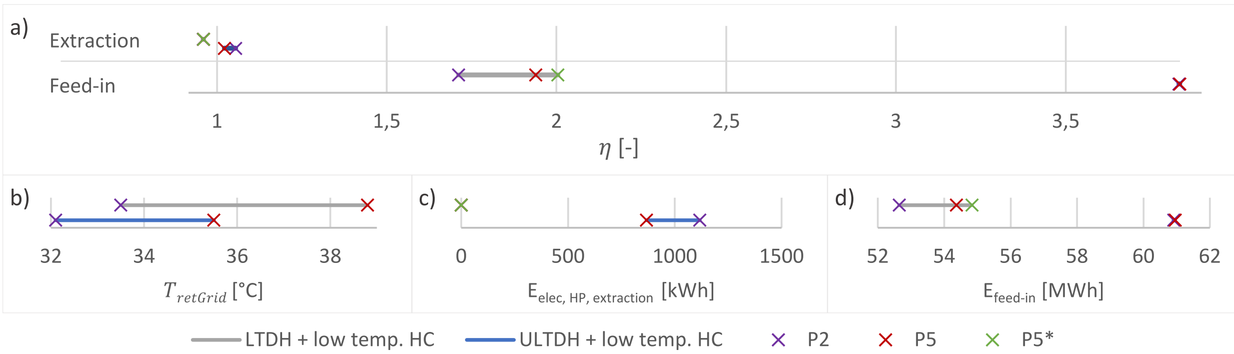


**Fig. 6.** Simulation results of the HP: Results lie in the range indicated by the different lines; the line color represents different scenarios; the possible configurations P2, P5 and P5* are marked separately. (a) shows the efficiency for the different operation phases 'extraction and 'feed-in', (b) shows the averaged return temperature during 'extraction', (c) the additional electric power necessary for the HP to heat up water to DHW temperature when the grid is too cold for 'extraction' and (d) shows the maximum feed-in potential during 'feed-in'. . (For interpretation of the references to color in this figure legend, the reader is referred to the web version of this article.)

The results show further that the main use case of the prosumer has to be chosen in advance in order to decide for the ideal configuration. If the prosumer extracts heat more often from the grid than it feeds in, P2 is the better choice. This configuration results in a lower return temperature on the grid side and a slightly higher efficiency. In a ULTDH grid, the HP however has to provide more additional heat to reach the DHW temperature level.

If the main purpose is to feed-in excess heat into a LTDH grid, P5/P5* is the better configuration. The efficiency, and feed-in potential is significantly higher in this case. P5* shows better results than P5, so it is advisable to use an additional 3WV. The results show that apart from increasing the efficiency due to the better layering, the feed-in criteria for switching off is exceeded less often.

For ST collectors, the simulation was done with a TS with an internal heat exchanger. This means, that only P2 and P5 are possible configurations. The results show, that both configurations show little difference in their efficiency and yield. The return temperature during extraction is, similar to the HP configuration, slightly better at P2.

Varying return temperatures on grid and house side showed for all types of HG that this shifts the results to a higher or lower level, but does not change the overall characteristics of the configurations.

Fig. 7 shows the daily feed-in potential of HP and CG and the average daily temperature over a time period of 20 days. It can be seen that the feed-in potential follows the temperature closely, since a high heat demand at low temperatures leaves only little capacity for feeding in heat. If a high feed-in potential during cold periods is required for the network, the HG should be oversized compared to dimensioning for standard operation.

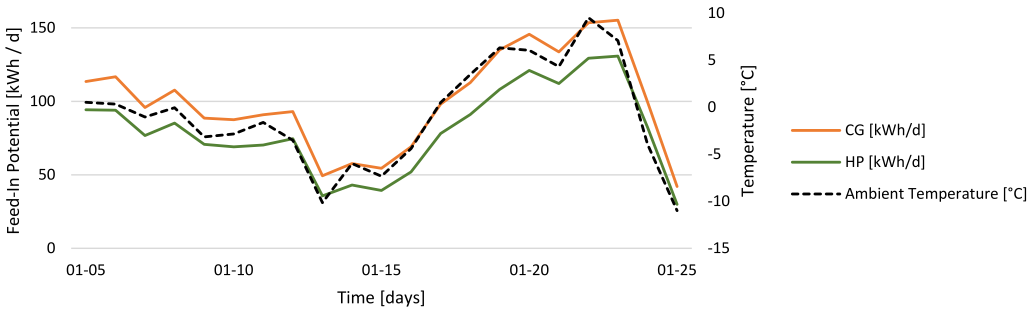


**Fig. 7.** Daily averaged feed-in potential of CG and HP in comparison with the ambient temperature.

## 6. Conclusion

The presented paper studies possible prosumer system configurations for HG, DH, TS and HC. The results provide an argumented decision guidance to select the most suitable prosumer side configuration for the desired HG, district heating network and consumption temperatures. Two configurations were identified in the scenario analysis, which in general suited best.

The configuration in which all components are directly connected to each other achieves the lowest return temperature and lowest storage losses. For a combustion-based HG, this leads to the highest efficiency due to the utilization of the condensation effect. This configuration also has the lowest return temperature on the heat grid side. This result reflects the best practice recommendations given by engineering offices and plumbers in the context of the planning of the CoSES laboratory environment at TU Munich [23]. It was recommended to use a completely parallel setup (P1). However, there are no reference papers or guidelines available on how to integrate thermal storages that would be suited to verify our results.

Since a direct connection of HP or ST with HC or DH is not possible, a different configuration must be chosen in which the HG is connected directly to the TS. At high grid temperatures, using of a 3WV between DH return flow and the inlet to the TS increases the efficiency of heat extraction from the network.

## Declaration of competing interest

The authors declare that they have no known competing financial interests or personal relationships that could have appeared to influence the work reported in this paper.

## Acknowledgments

This project was founded by the Federal Ministry for Economic Affairs and Energy, Germany (FKZ: 03EN3032A). The work of Vedran S. Perić was supported by Deutsche Forschungsgemeinschaft (DFG), Germany through “Optimal Operation of Integrated Low-Temperature Birdirectional Heat and Electric Grids (IntElHeat)” under project number 450821044.

## References

[1] Lund H, Möller B, Mathiesen BV, Dyrelund A. The role of district heating in future renewable energy systems. Energy 2010;35(3):1381–90. http://dx.doi.org/10.1016/j.energy.2009.11.023.

[2] Lund H, Werner S, Wiltshire R, Svendsen S, Thorsen JE, Hvelplund F, et al. 4th generation district heating (4GDH). Energy 2014;68:1–11. http://dx.doi.org/10.1016/j.energy.2014.02.089.
[3] Brand L, Calvén A, Englund J, Landersjö H, Lauenburg P. Smart district heating networks – A simulation study of prosumers' impact on technical parameters in distribution networks. Appl Energy 2014;129:39–48. http://dx.doi.org/10.1016/j.apenergy.2014.04.079.
[4] Kauko H, Kvalsvik KH, Rohde D, Nord N, Utne Å. Dynamic modeling of local district heating grids with prosumers: A case study for Norway. Energy 2018;151:261–71. http://dx.doi.org/10.1016/j.energy.2018.03.033.
[5] Brange L, Englund J, Lauenburg P. Prosumers in district heating networks – A Swedish case study. Appl Energy 2016;164:492–500. http://dx.doi.org/10.1016/j.apenergy.2015.12.020.
[6] Heymann M, Rühling K, Felsmann C. Integration of solar thermal systems into district heating – DH system simulation. Energy Procedia 2017;116:394–402. http://dx.doi.org/10.1016/j.egypro.2017.05.086.
[7] Fitó J, Hodencq S, Ramousse J, Wurtz F, Stutz B, Debray F, et al. Energy- and exergy-based optimal designs of a low-temperature industrial waste heat recovery system in district heating. Energy Convers Manage 2020;211:112753. http://dx.doi.org/10.1016/j.enconman.2020.112753.
[8] Rämä M, Wahlroos M. Introduction of new decentralised renewable heat supply in an existing district heating system. Energy 2018;154:68–79. http://dx.doi.org/10.1016/j.energy.2018.03.105.
[9] Zarin Pass R, Wetter M, Piette MA. A thermodynamic analysis of a novel bidirectional district heating and cooling network. Energy 2018;144:20–30. http://dx.doi.org/10.1016/j.energy.2017.11.122.
[10] Bünning F, Wetter M, Fuchs M, Müller D. Bidirectional low temperature district energy systems with agent-based control: Performance comparison and operation optimization. Appl Energy 2018;209:502–15. http://dx.doi.org/10.1016/j.apenergy.2017.10.072.
[11] Mangold D, Schäfer K. DEZENTRAL - Dezentrale einspeisung in nah- und fernwärmesysteme unter besonderer berücksichtigung der solarthermie teilbericht des verbundpartners solites forschungsbericht zum forschungsvorhaben 03et1039c laufzeit: 2012 Bis Mai 2015, solites. 2015, http://dx.doi.org/10.2314/GBV:866742697.
[12] Rosemann T, Löser J, Rühling K. A new DH control algorithm for a combined supply and feed-in substation and testing through hardware-in-the-loop. Energy Procedia 2017;116:416–25. http://dx.doi.org/10.1016/j.egypro.2017.05.089.
[13] Lamaison N, Bavière R, Cheze D, Paulus C. A multi-criteria analysis of bidirectional solar district heating substation architecture. In: SWC 2017 ISES solar world congress: international solar energy society. Freiburg im Breisgau: International Solar Energy Society (ISES); 2018, p. 1–11. http://dx.doi.org/10.18086/swc.2017.10.02.
[14] Paulus C, Papillon P. Substations for decentralized solar district heating: Design, performance and energy cost. Energy Procedia 2014;48:1076–85. http://dx.doi.org/10.1016/j.egypro.2014.02.122.
[15] DIN. Technische regeln für trinkwasser-installationen: teil 200: Installation typ a (geschlossenes system). Planung, Bauteile, Apparate, Werkstoffe: Technische Regel des DVGW; 2012, DIN 1988-200, accessed March 5, 2021.
[16] Lipp Josef Peter. Flexible Stromerzeugung mit Mikro-KWK-Anlagen: Experimentelle Untersuchung der Möglichkeiten einer flexiblen Stromerzeugung von Mikro-KWK-Anlagen mit Hilfe einer Wärmebedarfsprognose und einem intelligenten Speichermanagementsystem.
[17] Østergaard PA, Andersen AN. Booster heat pumps and central heat pumps in district heating. Appl Energy 2016;184:1374–88. http://dx.doi.org/10.1016/j.apenergy.2016.02.144.
[18] ratiotherm GmbH & Co. KG. Planning Guide for craftsmen, planners and architects.
[19] Zinsmeister D. Possible prosumer side configurations. 2021, http://dx.doi.org/10.13140/RG.2.2.25761.12642, Unpublished.
[20] Unger R, Schwan T, Mikoleit B, Bäker B, Kehrer C, Rodemann T. Green building - modelling renewable building energy systems and electric mobility concepts using modelica. In: Proceedings of the 9th international MODELICA conference, September 3-5, 2012, Munich, Germany. Linköping University Electronic Press; 2012, p. 897–906. http://dx.doi.org/10.3384/ecp12076897.
[21] RMB Energie. Operating Manual: Combined heat and power unit neoTower® LIVING CHP 2.0, CHP 3.3, CHP 4.0.
[22] Jordan U, Vajen K. Influence of the DHW load profile on the fractional energy savings. Sol Energy 2001;69:197–208. http://dx.doi.org/10.1016/S0038-092X(00)00154-7.
[23] Peric VS, Hamacher T, Mohapatra A, Christiange F, Zinsmeister D, Tzscheutschler P, et al. CoSES laboratory for combined energy systems At TU Munich. 1–5. http://dx.doi.org/10.1109/PESGM41954.2020.9281442.